

## Electronic Supplementary Information

### **Molecular dynamics simulation of carbon dioxide diffusion in NaA zeolite: assessment of surface effects and evaluation of bulk-like properties**

Sofia O. Slavova,<sup>ab</sup> Anastasia A. Sizova\*<sup>a</sup> and Vladimir V. Sizov<sup>a</sup>

a – Institute of Chemistry, St.Petersburg State University, 26 Universitetskii pr., 198504 St.Petersburg, Russia. E-mail: a.a.sizova@spbu.ru

b – Institute of General and Inorganic Chemistry, Bulgarian Academy of Sciences, 11 Acad. Georgi Bonchev str., 1113 Sofia, Bulgaria

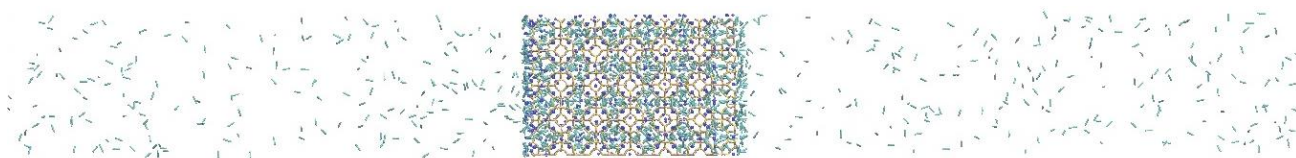


**Fig. S1** Simulation cell with zeolite LTA-4A and gas phase.

**Table S1** Force field parameters used for describing van der Waals interactions. The units are:  $C_6$  (kJ/mol·nm<sup>6</sup>),  $C_{12}$  (kJ/mol·nm<sup>12</sup>).

Sites	This work		[Phys. Chem. Chem. Phys. 15, 12882 (2013)]					
	$C_6$	$C_{12}$	non-fitted		CCFF		D2FF	
	$C_6$	$C_{12}$	$C_6$	$C_{12}$	$C_6$	$C_{12}$	$C_6$	$C_{12}$
C–C	$4.327 \cdot 10^{-4}$	$2.085 \cdot 10^{-7}$	$4.108 \cdot 10^{-4}$	$1.804 \cdot 10^{-7}$	$4.108 \cdot 10^{-4}$	$1.804 \cdot 10^{-7}$	$4.108 \cdot 10^{-4}$	$1.804 \cdot 10^{-7}$
C–O	$9.619 \cdot 10^{-4}$	$6.024 \cdot 10^{-7}$	$9.259 \cdot 10^{-4}$	$5.417 \cdot 10^{-7}$	$9.259 \cdot 10^{-4}$	$5.417 \cdot 10^{-7}$	$9.259 \cdot 10^{-4}$	$5.417 \cdot 10^{-7}$
O–O	$2.115 \cdot 10^{-3}$	$1.703 \cdot 10^{-6}$	$2.084 \cdot 10^{-3}$	$1.623 \cdot 10^{-6}$	$2.084 \cdot 10^{-3}$	$1.623 \cdot 10^{-6}$	$2.084 \cdot 10^{-3}$	$1.623 \cdot 10^{-6}$
C–O <sub>2</sub>	$1.110 \cdot 10^{-3}$	$2.630 \cdot 10^{-7}$	$1.110 \cdot 10^{-3}$	$2.630 \cdot 10^{-7}$	$1.026 \cdot 10^{-3}$	$1.088 \cdot 10^{-6}$	$1.080 \cdot 10^{-3}$	$1.166 \cdot 10^{-6}$
C–Al	$4.350 \cdot 10^{-3}$	$1.890 \cdot 10^{-6}$	$4.350 \cdot 10^{-3}$	$1.890 \cdot 10^{-6}$	$1.558 \cdot 10^{-3}$	$2.266 \cdot 10^{-6}$	$3.942 \cdot 10^{-3}$	$3.353 \cdot 10^{-6}$
C–Si	$4.020 \cdot 10^{-3}$	$2.030 \cdot 10^{-6}$	$4.020 \cdot 10^{-3}$	$2.030 \cdot 10^{-6}$	$3.723 \cdot 10^{-3}$	$8.379 \cdot 10^{-6}$	$3.922 \cdot 10^{-3}$	$9.004 \cdot 10^{-6}$
C–Na	$3.160 \cdot 10^{-3}$	$4.840 \cdot 10^{-7}$	$3.160 \cdot 10^{-3}$	$4.840 \cdot 10^{-7}$	$1.134 \cdot 10^{-3}$	$5.787 \cdot 10^{-7}$	$2.868 \cdot 10^{-3}$	$8.557 \cdot 10^{-7}$
O–O <sub>2</sub>	$7.000 \cdot 10^{-4}$	$1.310 \cdot 10^{-7}$	$7.000 \cdot 10^{-4}$	$1.310 \cdot 10^{-7}$	$6.485 \cdot 10^{-4}$	$5.398 \cdot 10^{-7}$	$6.831 \cdot 10^{-4}$	$5.797 \cdot 10^{-7}$
O–Al	$2.750 \cdot 10^{-3}$	$9.640 \cdot 10^{-7}$	$2.750 \cdot 10^{-3}$	$9.640 \cdot 10^{-7}$	$9.850 \cdot 10^{-4}$	$1.152 \cdot 10^{-6}$	$2.492 \cdot 10^{-3}$	$1.703 \cdot 10^{-6}$
O–Si	$2.540 \cdot 10^{-3}$	$1.040 \cdot 10^{-6}$	$2.540 \cdot 10^{-3}$	$1.040 \cdot 10^{-6}$	$2.354 \cdot 10^{-3}$	$4.283 \cdot 10^{-6}$	$2.481 \cdot 10^{-3}$	$4.608 \cdot 10^{-6}$
O–Na	$2.000 \cdot 10^{-3}$	$2.360 \cdot 10^{-7}$	$2.000 \cdot 10^{-3}$	$2.360 \cdot 10^{-7}$	$7.166 \cdot 10^{-4}$	$2.820 \cdot 10^{-7}$	$1.816 \cdot 10^{-3}$	$4.185 \cdot 10^{-7}$
Na–O <sub>2</sub>	$4.380 \cdot 10^{-3}$	$1.600 \cdot 10^{-6}$	<b>A*exp{-R/B} – C/R</b>		<b>A = 314702 kJ/mol, B = 0.02597 nm, C = 4380.5 kJ/mol</b>			

**Table S2** Parameters of charged interaction sites. Charges for the zeolite atoms are obtained from [Phys. Chem. Chem. Phys. 15, 12882 (2013)], charges for carbon dioxide are from [AIChE J. 47, 1676 (2001)].

Interaction Site	$q, e^-$
O	-1.3200
Si	2.2100
Al	2.0800
Na	0.9900
C <sub>CO2</sub>	0.6512
O <sub>CO2</sub>	-0.3256

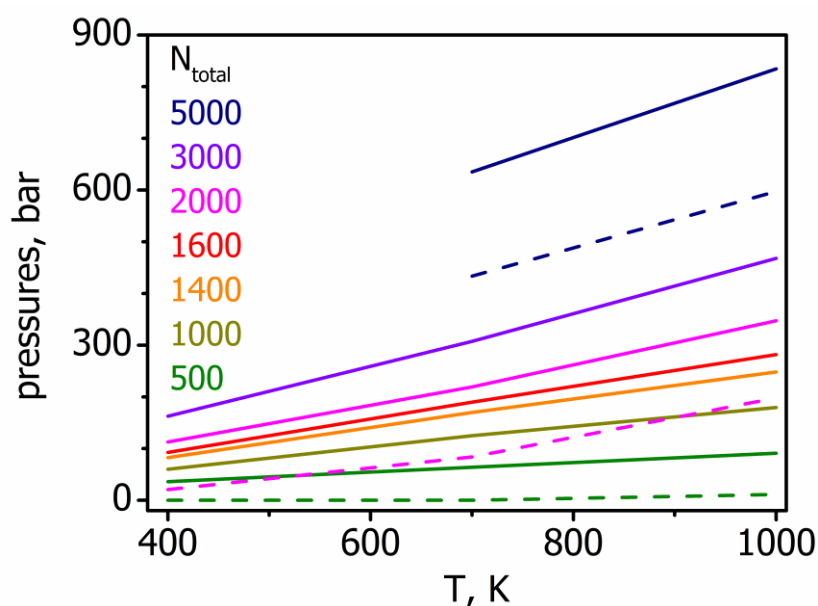


**Fig. S2** Initial (solid lines) and final (dashed lines) pressures in the reservoir. Notice the pressure drop accompanying the uptake of carbon dioxide from the reservoir.

### Background and details of techniques for the analysis of simulation data on diffusivity in zeolite with open surfaces

The diffusivity of carbon dioxide in cationic LTA is low, so a reliable evaluation of diffusion coefficients requires relatively long simulation times. This is particularly important for the calculation of local diffusion coefficients, since the time interval, over which the slope of MSD vs  $t$  dependence is being evaluated, may be long enough for a molecule to leave the region, which it had initially occupied. In this case, the calculated diffusion coefficient cannot be unambiguously assigned to a specific region of simulation cell. This problem is especially serious for the regions of porous material, which are located close to its external surface: some of the molecules may exit to the gas phase, where their mobility increases drastically, and then return back to the porous space of the simulated zeolite sample. Obviously, from the point of diffusivity studies, the behavior of such molecules will not be typical for confined gas, and the very high diffusion coefficients of such 'atypical' molecules are likely to contaminate the computed averages. Therefore, some kind of 'filtering' procedure has to be implemented in order to remove the data for 'atypical' molecules from the bulk of statistical data extracted from molecular dynamics trajectories. Such filtering can be position-based (i.e., monitoring of molecule trajectory ensures that it does not leave the specified volume during the time required for estimation of local diffusion coefficient) or mobility-based (i.e., monitoring of the computed diffusion coefficients for individual molecules filters out the marginal values). The implementation of a mobility-based filter results in the loss of information on the molecules with the highest kinetic temperatures. Therefore, upon comparison of diffusion coefficients calculated for the whole fragment of porous material with those obtained by averaging the pre-filtered local diffusion coefficients over the same fragment of zeolite, the former approach is very likely to yield somewhat higher values.

Another important point in data treatment techniques is the choice of bin width for the accumulation of statistics for local diffusion coefficients. While it is generally desirable to obtain a fine-grained diffusion profile, the corresponding decrease of bin width will come into collision with the abovementioned issue of relatively long time intervals used for calculation of diffusion coefficients. For small bin widths a considerable part of gas molecules may exit the monitored bin before a diffusion coefficient value can be obtained, and such molecules will be filtered out by position-based criteria. As a result, the statistics available for the averaging of diffusion coefficients will be seriously depleted. Moreover, the remaining data will reflect only the properties of those molecules, which do not leave the monitored bin at all, even though this behavior might be atypical for narrow bins. With these considerations in mind, the acceptable bin width was found to be comparable with a half of the unit cell size of LTA zeolite.

Values of the time intervals, over which the slope of MSD vs  $t$  dependence was determined, and bin widths are described in the main text.

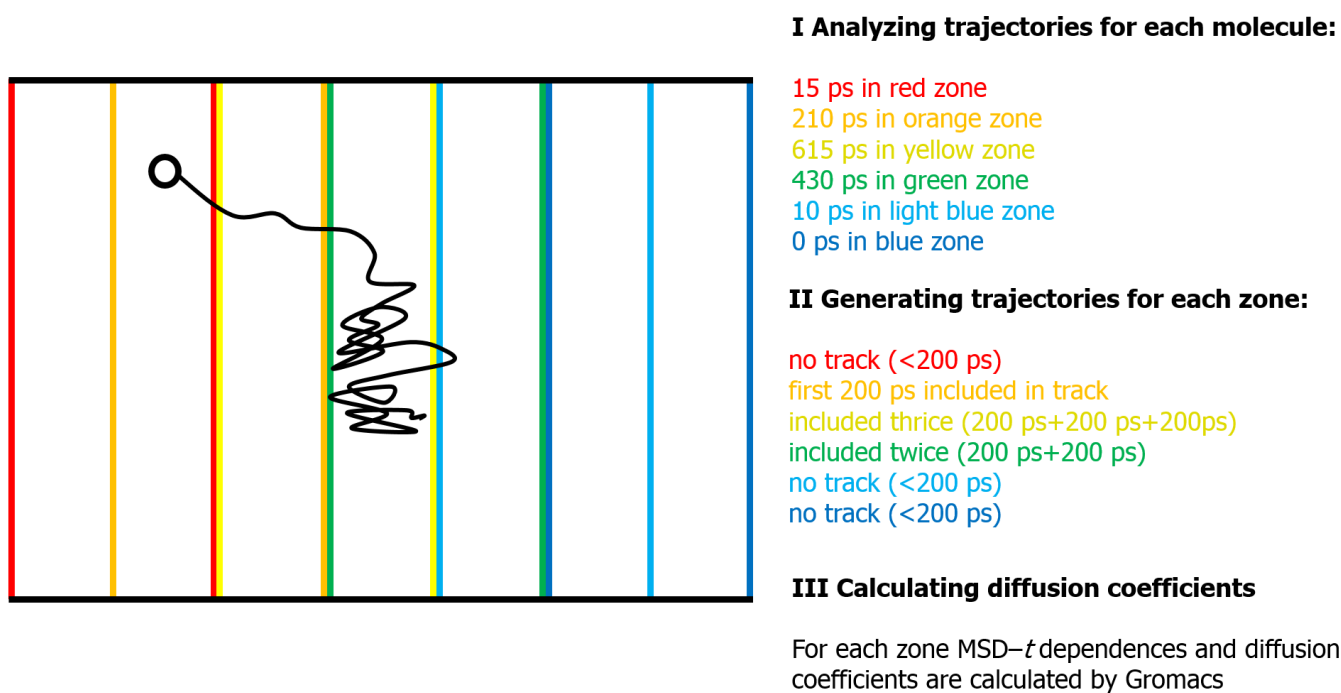


**Fig. S3** Scheme of trajectory analysis for multi-zone diffusion profiles.

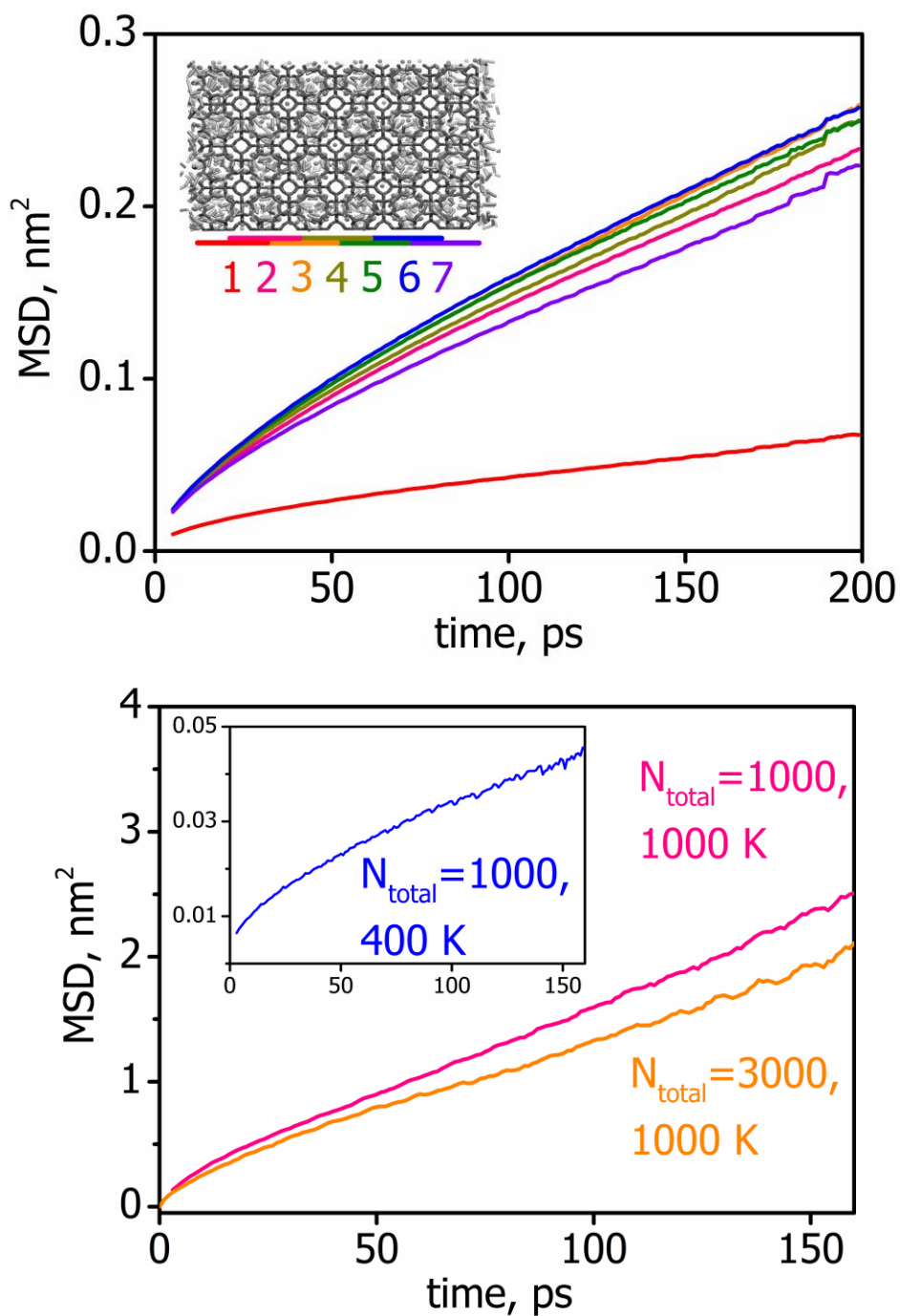


**Fig. S4** MSD vs time plots for ‘multi-zone’ approach used for evaluation of diffusion profile (upper) and ‘single-zone’ approach used for the bulk-like zeolite fragment (lower). The upper plot shows MSD for carbon dioxide molecules in seven overlapping zones (see inset) for a system containing a total of 1000  $\text{CO}_2$  molecules at 500 K. The lower plot shows MSD for various temperatures (400 K and 1000 K) and different total numbers of  $\text{CO}_2$  molecules (1000 and 3000).

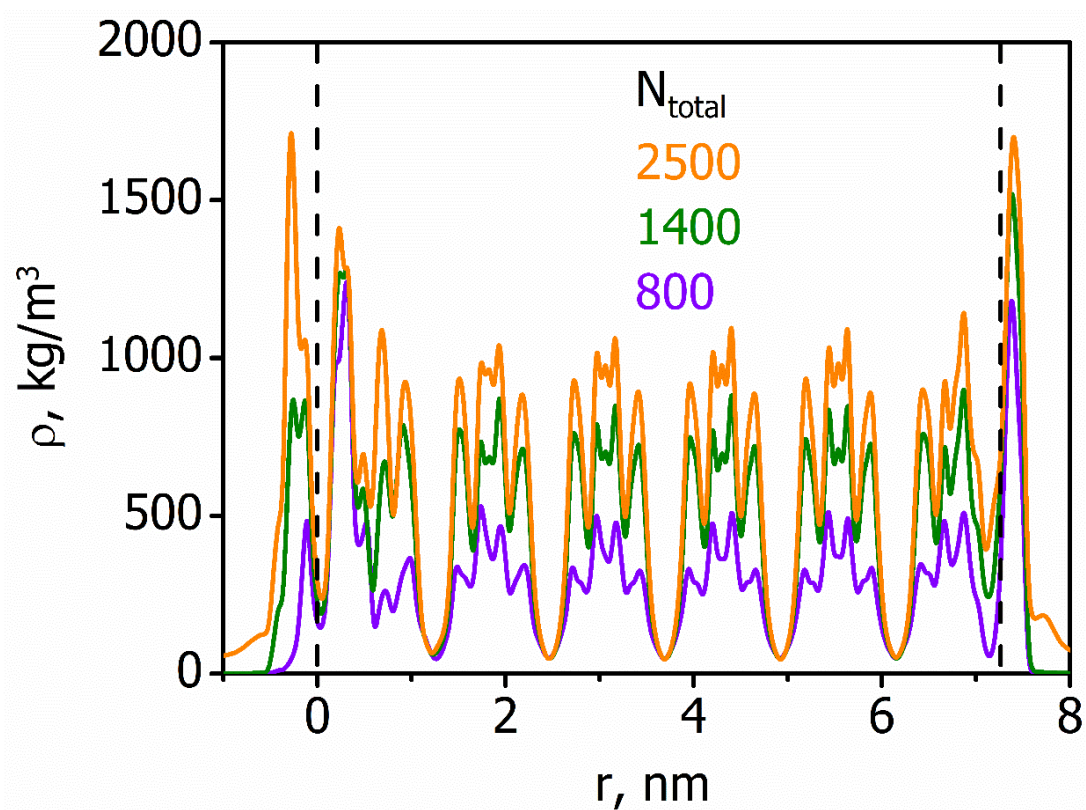


**Fig. S5** Local density profiles for centres of mass of carbon dioxide molecules adsorbed inside the zeolite fragment and at its external surfaces at 500 K. Dashed lines indicate the positions of the external surfaces.

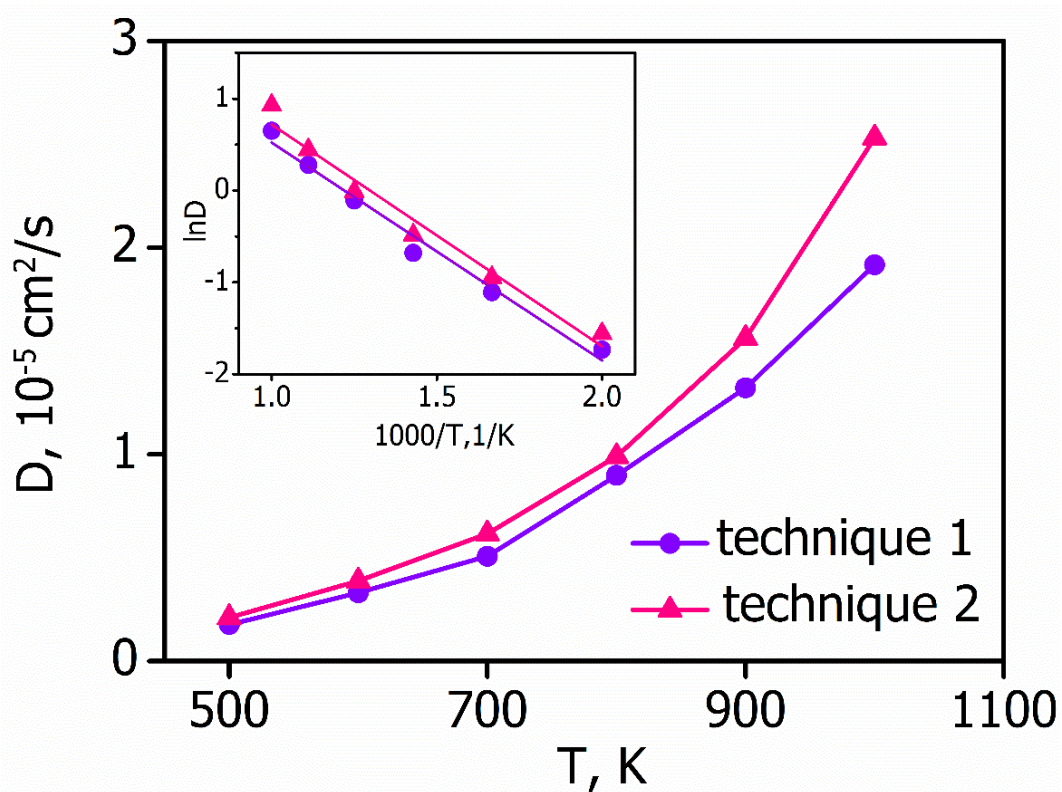


**Fig. S6** Comparison of diffusion coefficients obtained by profile-based (technique 1) and bulk-like (technique 2) approaches for the system with  $N_{total} = 1000$ . The inset shows the Arrhenius plot for both sets of data.



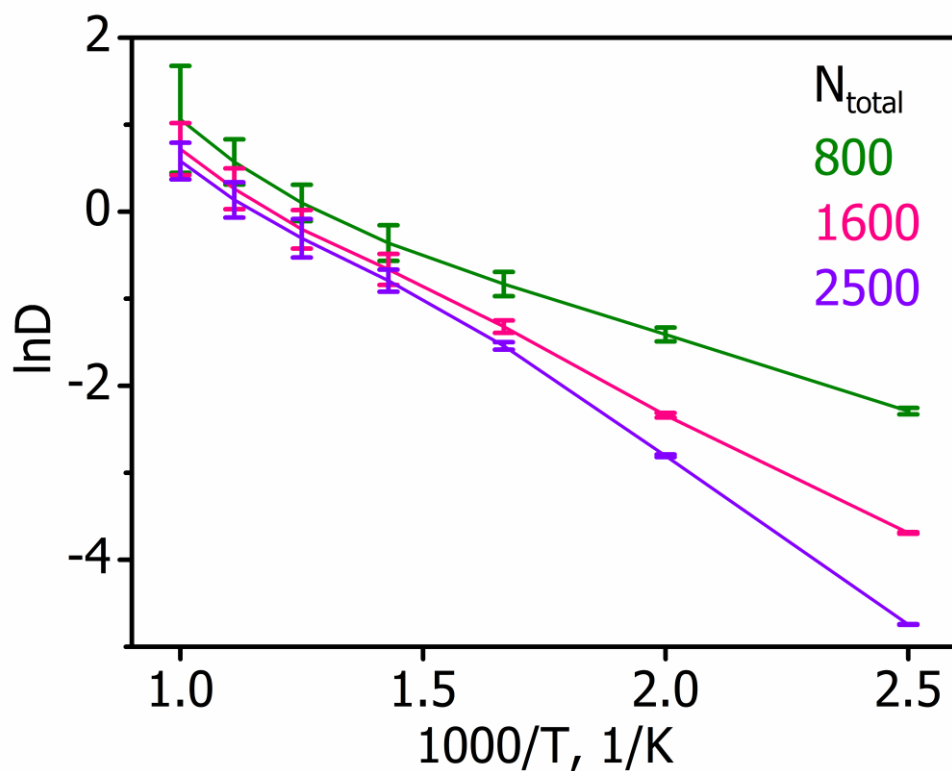


**Fig. S7** Arrhenius plots from Fig. 6 (main text) showing the error bars. The computational errors increase for higher temperatures (due to greater dispersion of properties) and lower CO<sub>2</sub> contents (due to lower quality of accumulated statistics).

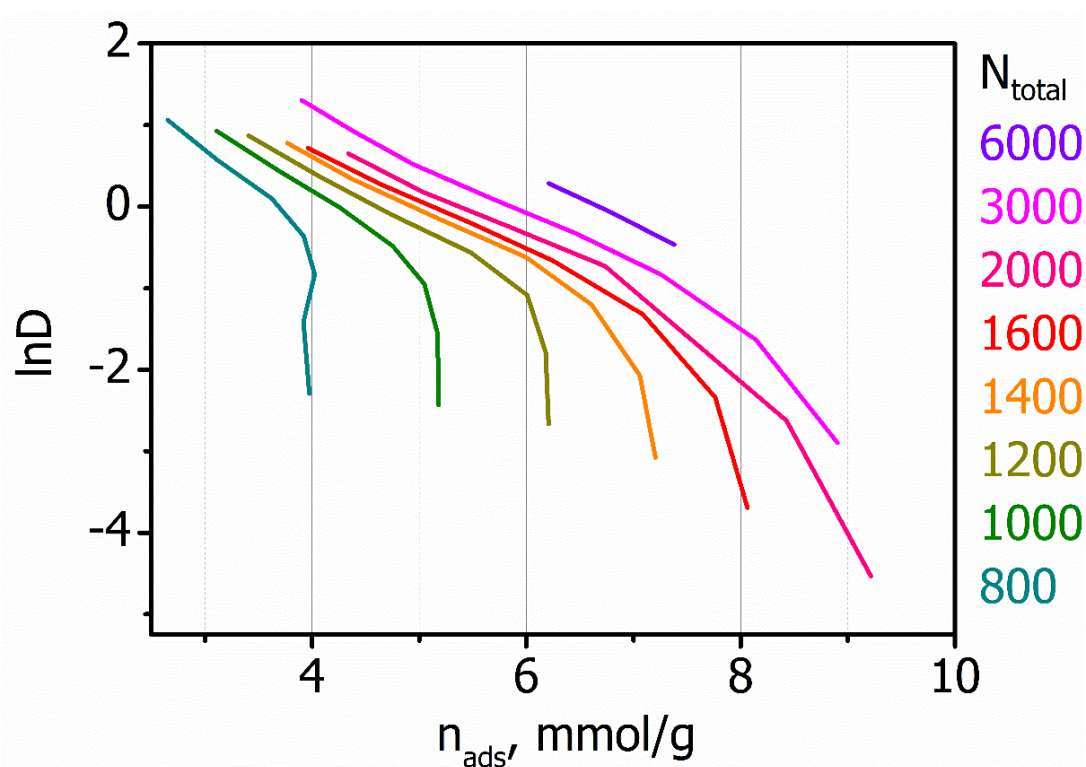


**Fig. S8** Dependence of the logarithm of CO<sub>2</sub> diffusion coefficient on the amount of CO<sub>2</sub> adsorbed in the central region of the zeolite for several  $N_{total}$  values (part of the data is omitted for clarity).

## On the evaluation of diffusion activation energy calculation from the diffusivity data at various temperatures and total amounts of gas in the system

Since the present computational approach called for molecular dynamics simulations for a fixed total number of gas molecules, the  $n_{ads}$  values could not be fixed, but rather had to be calculated. On the other hand, the large amount of computational data provides the means for reliable estimation of diffusivity at intermediate points, which were not directly covered by simulations. Such an estimation was based on the combination of Figs. 5 and 6. Both of these figures show multiple curves for different  $N_{total}$  values and share a common horizontal axis (inverse temperature). Taking advantage of these features, one can link any  $n_{ads}$  value from Fig. 5 with a diffusion coefficient for some  $1/T$  value from Fig. 6 using the following two-step procedure.

As the first step, Fig. 5 was used to locate the intersection points of horizontal lines corresponding to constant  $n_{ads}$  values with the computed  $n_{ads}$  vs  $1/T$  dependences for various  $N_{total}$ . Depending on  $n_{ads}$  value, one or several such intersection points could be obtained, with  $n_{ads}$  values ranging ca. 4.0 to 8.7 providing a sufficient number of points for subsequent analysis. Each of these intersection points can be described by three parameters:  $n_{ads}$ ,  $N_{total}$ , and  $1/T$ . Only two of these parameters are independent, so each point can be described by two parameters, e.g.,  $N_{total}$  and  $1/T$ . As the second step, the full set of selected  $\{N_{total}, 1/T\}$  points was transferred to Fig. 6, and horizontal lines were drawn to the  $\ln D$  axis to obtain the values of diffusion coefficients corresponding to each of these points. This resulted in a set of  $\{\ln D, 1/T\}$  points for each  $n_{ads}$  value (Fig. S8), which were then used to construct the Arrhenius dependences in Fig. 7.

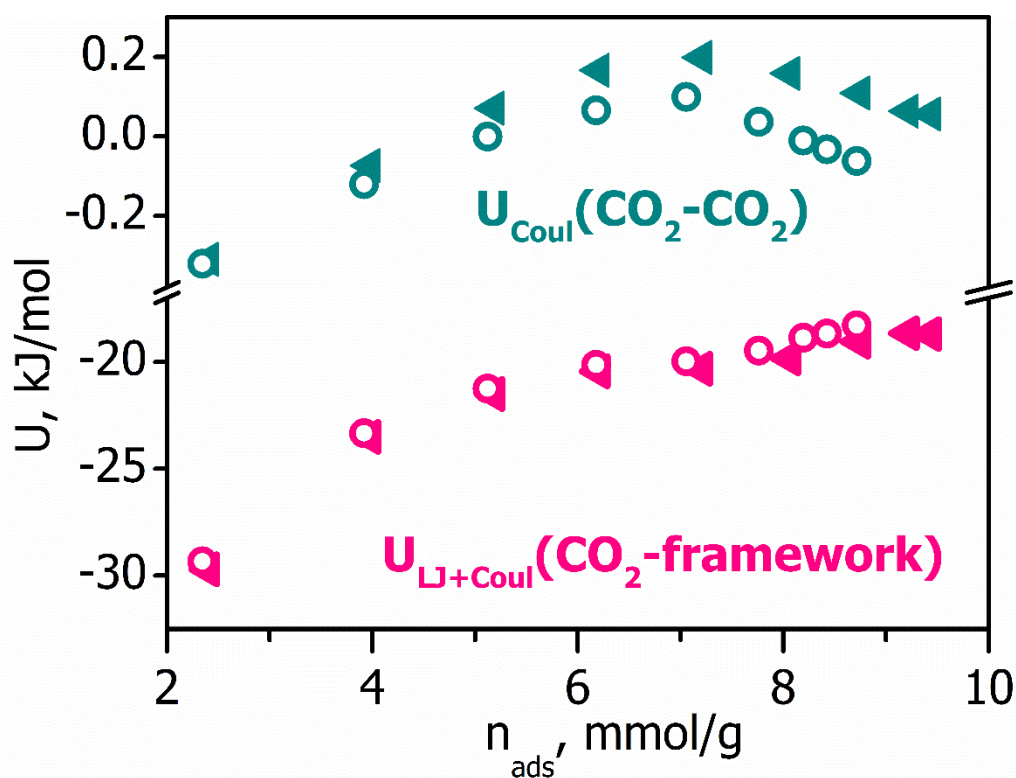


**Fig. S9** Dependence of interaction energies of adsorbed CO<sub>2</sub> with itself and with zeolite framework on the amount of adsorbed CO<sub>2</sub> at 400 K (triangles) and 500 K (circles).